Polaronic optical absorption in electron-doped and hole-doped cuprates

P. Calvani, M. Capizzi, S. Lupi, P. Maselli, and A. Paolone
Dipartimento di Fisica, Università di Roma "La Sapienza," Piazzale A. Moro 2, I-00185 Roma, Italy

P. Roy
Laboratoire pour l'Utilization de Rayonnement Electromagnétique, Université Paris-Sud, 91405 Orsay, France
(Received 11 April 1995; revised manuscript received 11 September 1995)

Polaronic features similar to those previously observed in the photoinduced spectra of cuprates have been detected in the reflectivity spectra of chemically doped parent compounds of high-critical-temperature superconductors, both *n* type and *p* type. In Nd_2CuO_{4-y} these features, whose intensities depend both on doping and temperature, include local vibrational modes in the far infrared and a broad band centered at $\sim$ 1000 cm^{-1}. The latter band is produced by the overtones of two (or three) local modes and is well described in terms of a small-polaron model, with a binding energy of about 500 cm^{-1}. Most of the above infrared features are shown to survive in the metallic phase of $Nd_{2-x}Ce_xCuO_{4-y}$, $Bi_2Sr_2CuO_6$, and $YBa_2Cu_3O_{7-y}$, where they appear as extra-Drude peaks. The occurrence of polarons is attributed to local modes strongly coupled to carriers, as shown by a comparison with tunneling results.

I. INTRODUCTION

In the long quest for an understanding of the mechanisms of high-temperature superconductivity, the optical properties of cuprates have been extensively studied, both in the normal and in the superconducting phases.[1] Electronic transitions which are common to different families of superconductors have been searched for and investigated. Three well defined structures have been identified in the reflectivity spectra: the charge-transfer (CT) band (in the visible range), the midinfrared (MIR) band, and the *d* band (both of which are in the midinfrared range).

The CT band is universally attributed to charge-transfer transitions between O $2p$ and Cu $3d$ states. It has been observed in the insulating phases of Y-Ba-Cu-O, Bi-Sr-(Ca,Y)-Cu-O, La-Sr-Cu-O, and *M*-Ce-Cu-O (M = Nd, Pr, Sm, Eu, Gd). The CT band appears to be associated with excitonic and polaronic effects.[2] Upon doping, either by chemical substitution or by photocarrier injection, it loses spectral weight in favor of another band, the MIR band, which appears inside the CT gap and is normally absent in stoichiometric samples.[3–5]

A number of experiments have been done, aimed at relating the insurgence of the MIR band to superconductivity. In particular, an inverse relation has been found to hold between the critical temperature and the MIR-band peak energy,[6,7] which suggests that high-T_c superconductivity is favored by a shift toward lower energy of the MIR band. This band indeed results from the overlap of two different components:[5,8] a contribution independent of temperature and centered in most compounds around 4000 cm^{-1}, and another contribution strongly dependent on temperature and peaked at $\sim$ 1000 cm^{-1}. The latter band, reported for both *e*- and *h*-doped systems,[5,8,9] is very similar to a structure observed in photoinduced absorption spectra of different compounds, and already shown to increase in strength with the critical temperature of the cuprate.[10–13] The shift observed in the MIR peak as the critical temperature (T_c) increases could then be explained by the growth of the 1000 cm^{-1} component. In $Nd_{2-x}Ce_xCuO_{4-y}$ (NCCO), the strength of this latter increases at 300 K with chemical doping and with the concentration of oxygen vacancies.[5,14] The 1000 cm^{-1} feature has therefore been attributed to transitions involving defects, whence its name, the *d* band. Nevertheless, a similar infrared band has been observed also in *h*-doped, oxygen-enriched La_2CuO_{4+y} (LCO), where both its line shape and temperature dependence are consistent with the absorption from a polaronic impurity state.[9] The polaronic origin of the *d* band has been firmly established in Nd_2CuO_{4-y} (NCO). Here the *d* band has been resolved and a relation between its fine structure and some extra-phonon peaks observed in the far infrared has been found to hold.[14,15] Furthermore, a broad spectrum of experimental techniques, ranging from extended x-ray absorption fine structure[16] to electron diffraction[17] and to neutron scattering[18] points toward the existence of polaron superstructures in superconducting cuprates as well as in nonsuperconducting perovskites. It has also been suggested[16] that such polaron ordering gives rise to unidimensional conductivity, thus enhancing the critical temperature of the material.

On the theoretical side, in the early 1980s Chakraverty[19] and Alexandrov and Ranninger[20] suggested that polarons would lead to high-T_c superconducting phases in ionic compounds. After the discovery of high-T_c superconductivity, several authors have again proposed that this phenomenon could be explained in terms of polaron-related models,[21–23] an issue still under discussion. The influence of polarons on the oxide optical properties has been analyzed in several theoretical works[24] after the early work of Holstein.[25] Recently, local modes coupled to electrons and holes have been predicted to show up in the normal-state phonon spectra of high-critical-temperature superconductors (HCTS's) for intermediate or large values of the electron-phonon interaction.[26] The optical conductivity in the presence of a strong electron-phonon interaction has been calculated by Emin[21] in terms of Reik's[24] standard polaron model, and by

TABLE I. Listing of the samples measured in the present experiment. They are all single crystals, except for sample 6 which is a highly oriented film, 2 μm thick, grown by liquid phase epitaxy.

Item	Material	Code	Doping y	Source	Comments
0	Nd_2CuO_{4-y}	MN8	~ 0	Univ. of Geneva	as grown
1	Nd_2CuO_{4-y}	MN24	<0.005	AT&T Bell Labs, M. H.	as grown
2	Nd_2CuO_{4-y}	MN22	>0	Univ. of Geneva	grown in reducing atm.
3	Nd_2CuO_{4-y}	MN19	0.04	Univ. of Geneva	annealed in N_2, 900 °C, 10–15 h
4	Gd_2CuO_{4-y}	MG01	<0.005	AT&T Bell Labs, M. H.	as grown
5	$Bi_2Sr_2YCu_2O_{8+y}$	MBY1		Univ. of Lausanne	
6	$Bi_2Sr_2CuO_6$	FBP4		Univ. of Rome II	as grown
7	$Bi_2Sr_2CuO_6$	M4B		Univ. of Lausanne	as grown

Alexandrov *et al.* by the exact solution of a finite size Holstein model.[27]

This paper is aimed (i) at providing clear evidence of polarons in both hole- and electron-doped cuprates, (ii) at showing that they survive in the metallic phase, and (iii) at looking for hints of their relevance in the superconducting mechanism. This will be done by discussing reflectivity measurements in the far and midinfrared on different cuprates, as well as by a careful reanalysis of optical and transport results obtained by different authors. In particular, it will be shown that the additional far-infrared modes observed here in slightly *e*- and *h*-doped compounds correspond to the extra-Drude features observed by several authors in the corresponding superconductors. It will also be shown that the extra-phonon features determined from the far-infrared reflectivity in insulating NCO correspond to peaks in the spectral function $\alpha^2F(\omega)$, as obtained by tunneling measurements[28] in superconducting $Nd_{2-x}Ce_xCuO_{4-y}$.

II. EXPERIMENT

Several *e*-doped and *h*-doped single crystals have been studied, as listed in Table I. The NCO samples were prepared by different procedures, in order to obtain crystals with different concentrations of oxygen vacancies. Sample 0, prepared at the University of Geneva, is stoichiometric. Sample 1, prepared at AT&T Bell Labs of Murray Hill, is as grown and nearly stoichiometric ($y<0.005$). Samples 2 and 3, prepared at the University of Geneva, were reduced during and after their growth, respectively (see Table I and Ref. 14). The samples were mounted on the cold finger of a two-stage closed-cycle cryostat, whose temperature was kept constant within $\pm$ 2 K and could be varied from 300 to 20 K. The reflectivity $R(\omega)$ of all samples, relative to gold- and aluminum-plated references, has been measured with the electric field polarized in the *a*-*b* plane. Data were collected in two different laboratories by rapid scanning interferometers, typically from 100 through 25 000 cm^{-1}. The real part of the optical conductivity $\sigma(\omega)$ has usually been obtained from canonical Kramers-Kronig transformations. A Drude-Lorentz fit has been used to extrapolate the reflectivity data beyond the measured range. The same fitting procedure has been used to extract oscillator energies, linewidths, and intensities from the experimental $\sigma(\omega)$.

III. RESULTS AND DISCUSSION

The reflectivity spectra of the *d* band, taken at different temperatures, are reported in Fig. 1 between 100 and 1200 cm^{-1} for three NCO single crystals. The corresponding optical conductivities, as obtained by a standard Kramers-Kronig analysis, are shown in Fig. 2. The *d* band depends on doping at room temperature, while it is roughly constant at low *T*. In all samples, and *over the whole energy range*, the reflectivity increases with decreasing temperature, even if the intensity at high frequency saturates at roughly 200 K, as shown in Fig. 1(b). In the following subsections we shall separately examine the spectral regions below 600 cm^{-1} and above 600 cm^{-1} for slightly doped, insulating cuprates. Then we shall extend the discussion to their metallic phases.

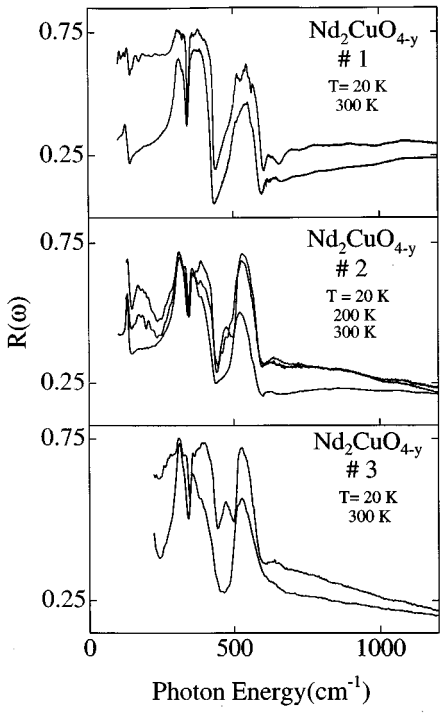

FIG. 1. The reflectivity $R(\omega)$ of three Nd_2CuO_{4-y} single crystals (1–3) in the far- and midinfrared region, at different temperatures. The oxygen deficiency y increases from top to bottom.

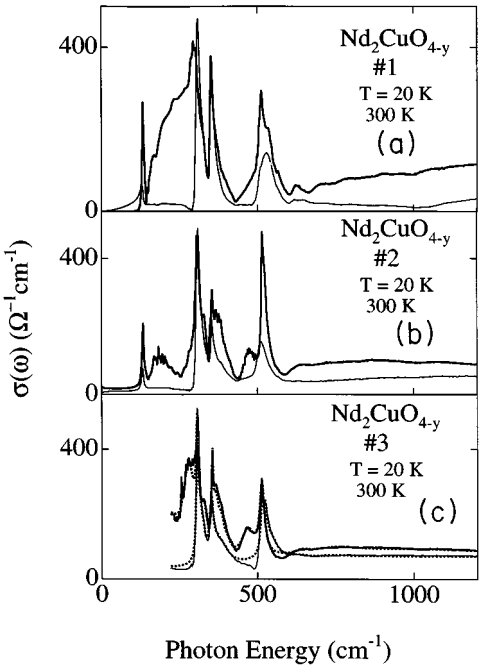

FIG. 2. The optical conductivities corresponding to the reflectivity data of the three NCO samples reported in Fig. 1 (thin solid lines correspond to $T = 300$ K, thick solid lines to $T = 20$ K). The dotted lines in (c) are the result of a best fitting procedure in terms of Lorentz oscillators for the extended and local modes, and of a Gaussian line shape for the *d* band.

A. The insulating phase: The *d* band

1. Description in terms of a standard polaron model

The data of Fig. 1, already partially reported in Ref. 14, will be here reanalyzed in order to support the polaronic origin of the band at 1000 cm^{-1} (*d* band). Indeed, a polaronic origin is consistent with the temperature dependence of the linewidth Γ_d of this band. According to a conventional adiabatic approach,[29] a small-polaron absorption is described by a single Gaussian with a linewidth Γ_d given by

$$\Gamma_d = \hbar\omega^* [8 \ln 2 S \coth(\hbar\omega^*/2kT)]^{1/2}, \qquad (1)$$

where S, the Huang-Rhys factor, is a measure of the electron-phonon interaction, and ω^* is an average phonon energy. The optical conductivity $\sigma(\omega)$ of the strongly doped sample 3 in Fig. 2(c) has been fitted at different temperatures by using both Lorentzian line shapes (for the far-infrared oscillators up to 700 cm^{-1}, see Sec. III B), and a single Gaussian (for the broad *d* band). The fitting curves for $T = 20$ K and $T = 300$ K are shown as dotted lines in Fig. 2(c). The resulting values for the *d*-band width Γ_d are reported in Fig. 3, as well as their best fit to Eq. (1) (solid line). One may notice that Eq. (1) well reproduces the ''saturation'' observed at low temperature in the change of the linewidth. The Huang-Rhys factor S turns out to be 4.4 ± 0.4, indicating that the electron-phonon interaction ranges from medium to strong. The average phonon energy ω^* is 210 ± 10 cm^{-1}. Under the same standard approach, to first order the peak energy E_{peak} of the polaron band is simply $E_i + S\hbar\omega^*$, where E_i is the binding energy of the impurity which provides the free carriers (here, an oxygen vacancy). In the present case,

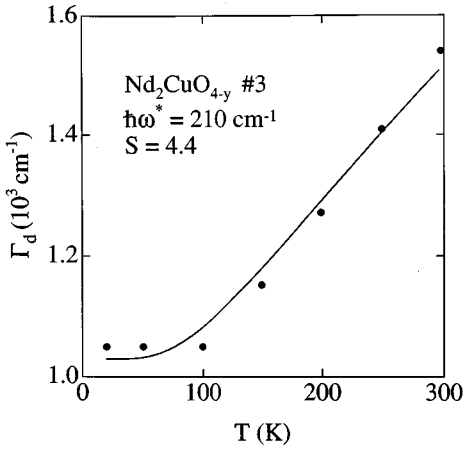

FIG. 3. The width Γ_d of the *d* band is plotted for the most doped Nd_2CuO_{4-y} sample 3 as a function of temperature. The solid line is the best fit of Eq. (1) to data. The average phonon energy ω^* and the Huang-Rhys factor S are given.

from the data of Figs. 2 and 4(a) $E_{peak} \sim 800$ cm^{-1} in sample 3, which gives $E_i \simeq 0$ by using the above values for S and ω^*. In photoinduced absorption experiments on NCO, where carriers are not bound to impurities, one finds[11] a band with $E_{peak} \sim 1280$ cm^{-1}, consistent with the values found, here and elsewhere,[8] in samples with low chemical doping. This indicates that (i) E_{peak} depends on doping, as confirmed in Figs. 2 and 4(a); (ii) the impurity binding energy vanishes for both photoinduced and chemically induced carriers. As

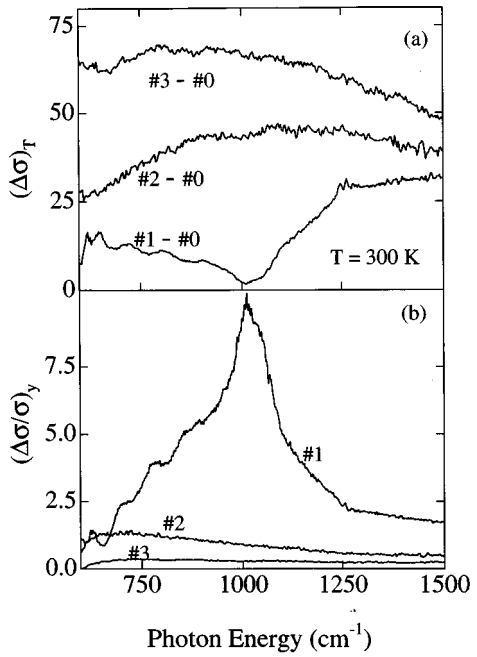

FIG. 4. (a) The difference $(\Delta\sigma)_T = \sigma(\omega,300,y) - \sigma(\omega,300,0)$ is plotted for the reduced samples 1, 2, and 3 ($y > 0$) relative to the as-grown sample 0 ($y = 0$), in order to subtract the high-energy contributions. (b) $(\Delta\sigma/\sigma)_y = [\sigma(\omega,20,y) - \sigma(\omega,300,y)]/\sigma(\omega,300,y)$ is reported for three Nd_2CuO_{4-y} samples, in order to show the different behaviors with temperature of the *d* band in crystals with different doping.

TABLE II. Peak energies, in cm^{-1}, of the spectral features observed in the reflectivity spectra of a variety of insulating slightly doped cuprates. In the case of NCO, the peak energies of the local modes have been obtained by a best fit of optical conductivity data. For NCO, a tentative assignment of the local modes is also given in terms of three series of overtones, as explained in the text.

NCO 0	NCO 1	NCO 2, 3	n_1	n_2	n_3	GCO 4	BSYCO 5
Local mode							
		165	1				
		282±4		1			
		327	2				
		366			1		
		383			1		
		471	3				
		507					
		522					
		536		2			
		550		2			
	630	641	4			635	
	710	717±7			2	715	715
	780	782	5	3		800	790
	855	861±2				870	865
	895						
		960±3	6				
	1020			4			
Phonon mode							
132		132					
309		305					
352		354					
511		514					

far as the dependence on temperature of the *d*-band intensity is concerned, the growth of this latter for decreasing T (with a saturation at $T \approx 200$ K) is also explained by the conventional adiabatic approach and is compatible with a small-polaron model (the intensity of large polarons is predicted to be independent of temperature[21]).

It is worth noticing that results similar to those presented here are obtained whenever a polaronic one-phonon model is applied to infrared bands observed at $\sim 1000\ cm^{-1}$. Photoinduced absorption measurements in $YBa_2Cu_3O_{6.3}$ and $Tl_2Ba_2Ca_{0.98}Gd_{0.02}Cu_2O_8$ yielded $\omega^* \simeq 200\ cm^{-1}$ in both compounds, with $S = 7$ and $S = 5.6$, respectively.[12] Conversely, reflectivity measurements in La_2CuO_4 gave $\omega^* \simeq 350\ cm^{-1}$, from an analysis of the T dependence of the charge-transfer gap in terms of a Fröhlich polaron,[2] and $S = 2.5$ from a line shape fit of the *d* band.[9]

The dependence of the *d* band on doping and temperature is evident in Fig. 2. Therein, one may observe that the *d*-band intensity at room temperature grows with doping from (a) to (c), while it does not change appreciably at low T. This is more evident in Fig. 4, where the differences

$$(\Delta\sigma)_T = \sigma(\omega,T,y) - \sigma(\omega,T,0)$$

evaluated at $T = 300$ K for samples 1, 2, and 3 relative to sample 0 are plotted. Sample 0 is the most stoichiometric crystal available ($y = 0$), as confirmed by the absence of any sizable *d*-band contribution. Figure 4(a) shows the insurgence upon doping of a *d* band, whose peak moves toward low energy as doping increases from sample 1 to sample 3.[30,31] At low doping, the peak is placed above $1200\ cm^{-1}$ at $T = 300$ K, in agreement with previous determinations,[8] while a minimum is observed at $\sim 1000\ cm^{-1}$. This minimum, whose origin is not clear, is observed only in sample 1 and rapidly disappears on going to low temperature. This can be better seen in Fig. 4(b) where the dependence of the *d* band on temperature is shown by reporting the normalized difference

$$(\Delta\sigma/\sigma)_y = [\sigma(\omega,20,y) - \sigma(\omega,300,y)]/\sigma(\omega,300,y)$$

evaluated at fixed oxygen concentration for all samples. As one can see, the nearly stoichiometric sample 1 shows the highest $(\Delta\sigma/\sigma)_y$, while for the strongly doped samples this quantity is very small. In turn, samples 2 and 3 show a shift of spectral weight to lower energies as temperature decreases, similar to that observed above for increasing doping.

2. Departure from a standard polaron model

In the low-doping regime, sample 1 in Figs. 2 and 4, infrared active vibrations (IRAV's) appear on the top of the *d* band. The energies of the IRAV's are reported in Table II. The observation of a fine structure with peaks separated by energies of the order of those of the lattice vibrations provides further evidence for the polaronic origin of the *d* band. Indeed, it has been recently shown[27] that infrared bands ex-

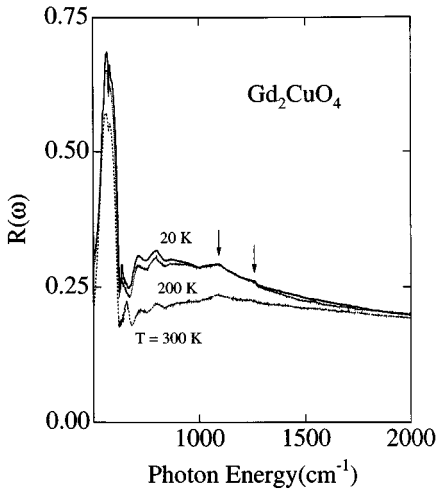

FIG. 5. The midinfrared reflectivity $R(\omega)$ for an as-grown Gd_2CuO_4 single crystal at three different temperatures. Low-T spectra show a d band partially resolved into peaks. The features indicated by arrows are instrumental.

hibiting IRAV's like those in Fig. 4 are consistent with calculations of the polaron optical conductivity by a finite size Holstein model, when the conventional adiabatic approximation is abandoned. In fact, the theoretical $\sigma(\omega)$ exhibits a number of peaks which are separated by phononlike energies and have different spectral weights according to the number of phonons involved.

Although we have discussed in detail the e-doped cuprate family, the insurgence of a polaronic d band with IRAV's is quite general, as shown in Figs. 5 and 6. Therein, the midinfrared spectra of two insulating samples belonging to different cuprate families are shown for different temperatures. In Fig. 5, the midinfrared spectra of an as-grown Gd_2CuO_4 (GCO) single crystal are reported for different temperatures. This sample also exhibits a well defined d band extending up to $\approx$ 2000 cm^{-1}, whose intensity strongly increases for decreasing temperature and nearly saturates at 200 K, as in NCO. The energies of the IRAV's on the top of the d band are reported in Table II.

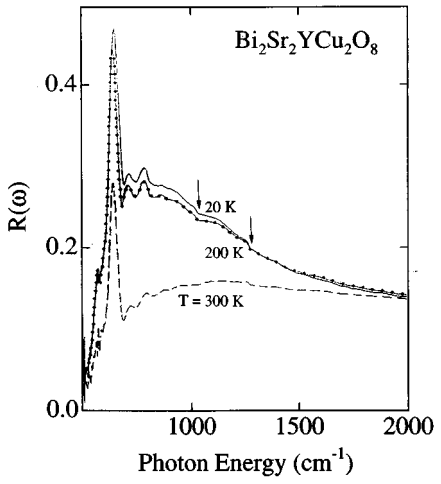

FIG. 6. The midinfrared reflectivity $R(\omega)$ of an as-grown $Bi_2Sr_2YCu_2O_8$ single crystal, at three different temperatures. As in Fig. 4, low-T spectra show several peaks in the d band. The small dips indicated by arrows are instrumental.

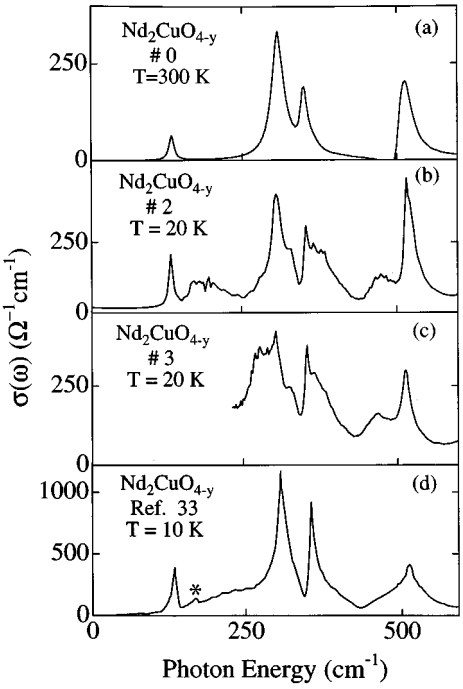

FIG. 7. The real part $\sigma(\omega)$ of the optical conductivity of four Nd_2CuO_{4-y} samples. The spectrum in (d) results from a reelaboration of data reported in Ref. 33.

The midinfrared reflectivity of a single crystal of insulating $Bi_2Sr_2YCu_2O_8$ (BSYCO) is shown in Fig. 6 for three different temperatures. The spectra in Fig. 6 are affected by a large uncertainty in the absolute intensity values, due to the small dimensions of the sample. However, together with a phonon peak[32] at 637 cm^{-1}, one may observe a well defined d band with a few peaks on the top. Their energies are reported in Table II.

In conclusion, d bands with IRAV's on their top are observed in both Gd_2CuO_{4-y} and $Bi_2Sr_2YCu_2O_8$, at energies corresponding to those found in Nd_2CuO_{4-y}. This supports a common origin for polarons in these materials, whose composition is completely different except for having Cu-O planes. In the following subsection, a relation will be established between the energies of the peaks resolved in the d band and those of the extra-phonon modes induced by doping and detected in the same spectra at lower energies.

B. The insulating phase: Local vibrational modes

The far-infrared, room-temperature $\sigma(\omega)$ of the NCO stoichiometric sample 0, already published in a previous paper,[5] is reported in Fig. 7(a) for the reader's convenience. It represents a good example of a "purely phononic" far-infrared spectrum, where only the four infrared-active E_u phonons predicted by group theory for the T' structure of NCO are detected. Their energies are reported in the bottom part of Table II. The far-infrared $\sigma(\omega)$ at 20 K is presented in Figs. 7(b) and 7(c) for the NCO crystals 2 and 3, respectively. In Fig. 7(d), $\sigma(\omega)$ is instead reported at 10 K for a NCO sample

annealed under Ar atmosphere and measured by different authors.[33] The plot has been obtained by multiplying by $\omega/(4\pi)$ the imaginary part of the dielectric function ϵ_2, as reported in Fig. 1 of Ref. 33.

By a first inspection of Fig. 7, one sees that the four E_u phonon peaks of Fig. 7(a) evolve into four bands when passing to the low-temperature spectra of the doped samples [Figs. 7(b) to 7(d)]. Those bands are structured and in no way can be reduced to single-phonon modes, even if they are centered roughly at the energies of the four E_u vibrations.

In addition, one observes at low T a broad background between 180 and 250 cm^{-1}. Its intensity increases as temperature is lowered but decreases for increasing doping. The latter feature shows that the origin of this background, which will not be discussed further on, is not related to excess charges.

A weak peak at 165 cm^{-1} barely emerges from the background in Fig. 7(b), while it is more clear in Fig. 7(d) (see asterisk) as well as in the spectrum at 10 K of a NCO single crystal reported in Fig. 3 of Ref. 34. It has been attributed to magnetic effects in Ref. 33, and to disorder-induced effects in Ref. 34. It should be mentioned that neutron scattering data show a transition at 165 cm^{-1}, which has been attributed to a crystal field splitting[35] in the electronic levels of the Nd^{3+} ion. However, this transition is not expected to be infrared active and it has not been observed[36] in stoichiometric samples down to $T = 10$ K. This rules out the hypothesis of a magnetic origin.

An explanation for the 165 cm^{-1} peak should then be searched for in the context of the profound modifications induced by doping on the phonon spectrum. Indeed, at low T a number of IRAV's add to the E_u phonon peaks in the reduced crystals 2 and 3, as well as in the far-infrared spectra at low T of Refs. 33 and 34 (not discussed by the authors). These IRAV modes are similar to the photoinduced local modes (PILM's) observed by optical injection of charges.[10–13,37] This rules out the possibility that the IRAV's observed in the present, chemically doped, crystals might be simply due to point defects, e.g., oxygen vacancies.

The attribution of the IRAV bands in Fig. 7 to local modes[14] is supported by the following arguments.

The energies of the IRAV's show just a few accidental correspondences with the infrared longitudinal modes of the stoichiometric compound,[5] or with the Raman-active modes[33] of the a-b plane in the same material. Moreover, the high orientation of the present single crystals excludes the possibility of direct contributions from c-axis vibrations. Fano antiresonances between some c-axis phonons and the electronic continuum of the a-b plane[38] can also be excluded, due to the absence of any sizable Drude contribution in the present NCO samples at low T. On the other hand, the IRAV's of Fig. 7 can be distinguished from the four E_u phonons of the a-b plane by their increase with doping[14,36] (in NCO with the oxygen deficiency y) and their decrease with temperature between 200 and 300 K (at $T < 200$ K the intensity of most extra modes remains constant).[14] This suggests that the IRAV's may arise from lattice distortions induced in the polar lattice of NCO by the excess charges created by doping. Recent calculations in Cu-O clusters doped by holes show that the total energy is minimized when the hole resides on a Cu atom and the four nearest neighbor O atoms move toward the Cu atom.[26] This doping-induced lattice distortion gives rise to new infrared-active (local) modes. They will appear as satellite bands on both the low- and the high-energy sides of the unperturbed lattice phonons, with intensities which increase with the strength of the hole-phonon interaction.[26]

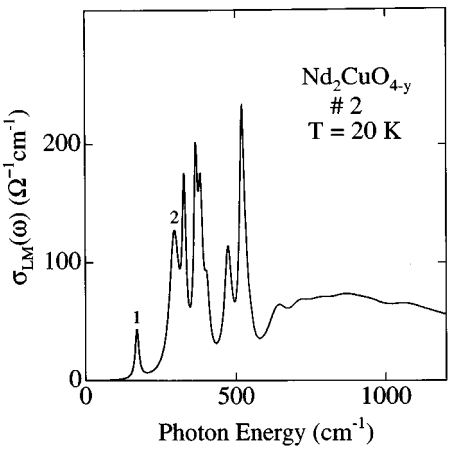

FIG. 8. $\sigma_{LM}(\omega)$, obtained for the doping-dependent additional modes only, is plotted for sample 2 at 20 K. The fundamental modes 1 (165 cm^{-1}) and 2 (282 cm^{-1}) are indicated.

On the grounds of the above considerations, in the strongly doped samples the optical conductivity $\sigma(\omega)$ can be split into three contributions:

$$\sigma(\omega)=\sigma_{ph}(\omega)+\sigma_{bgd}(\omega)+\sigma_{LM}(\omega)$$

where $\sigma_{ph}(\omega)$ is the phonon term and $\sigma_{LM}(\omega)$ is that of the local modes (LM's). $\sigma_{bgd}(\omega)$ is the contribution from the broad background around 200 cm^{-1}. As already stated, this latter depends on doping in the opposite way to that found for the local modes. The oscillator parameters have been obtained by a Drude-Lorentz fitting procedure.[5] The oscillator energies, listed in Table II, result from an average over the Nd_2CuO_{4-y} samples 2 and 3. Most of these values can be interpreted in terms of overtones or combination bands of two fundamental modes, as explained in the following.

The local-mode conductivity $\sigma_{LM}(\omega)$ at 20 K is reported in Fig. 8 for sample 2. Several bands are well resolved, whose peak energies have been partially reported previously.[14,39] Surprisingly, in both samples 2 and 3, the total intensity of LM's is roughly twice as much as the total intensity of the four E_u phonons. It has already been mentioned that these IRAV's show a dependence on doping and temperature similar to that found for the d band. It is therefore most likely that these modes are the low-order elements of a polaron series whose convolution gives rise to the d band. The structures still observed on the top of this band at intermediate doping, see 2, would then be the remnants of overtone and combination bands of a few of these far-infrared LM's. Higher-energy overtones would be too broad to be resolved.

The two lowest-energy LM's provide the basis for a simple model which (i) accounts for most of the far-infrared and the d-band IRAV's, (ii) confirms the interpretation of the spectrum in terms of small polarons, and (iii) provides a few characteristic parameters of the polaron. The two lowest LM

energies,[40] $\omega_1 = 165\ \mathrm{cm}^{-1}$ and $\omega_2 = 287\ \mathrm{cm}^{-1}$, lead to a mean value $\omega^* = (I_1\omega_1 + I_2\omega_2)/(I_1 + I_2) = 260 \pm 10\ \mathrm{cm}^{-1}$ at 20 K in sample 2. This value may be compared with that ($210 \pm 10\ \mathrm{cm}^{-1}$) obtained above by fitting to Eq. (1) the *d*-band linewidth of sample 3 derived in a single-phonon approach.

Within the adiabatic model, the (thermal) binding energy E_p of the small polaron, as described by a standard single-phonon calculation, can be estimated. The optical conductivity is then given by Reik's formula[24]

$$\sigma(\omega) \propto [t^2/(2E_pT)][(1-e^{-\omega/T})/\omega] \times \exp[-(\omega - 2E_p)^2/(8E_pT)], \quad (2)$$

where t is an intersite hopping frequency. According to Eq. (2), for $T \to 0$ the maximum absorption will occur at $\omega \simeq 2E_p$, namely, at $\omega \simeq n\omega^*$ ($n > 1$ is the number of phonons of energy ω^* which best approximates the Huang-Rhys factor S). From an inspection of Fig. 4(a), where the *d*-band peak moves to low energy for increasing doping, E_p turns out to be $> 600\ \mathrm{cm}^{-1}$ in sample 1, $\sim 550\ \mathrm{cm}^{-1}$ in sample 2, and $\sim 400\ \mathrm{cm}^{-1}$ in the most heavily doped sample 3. Alternatively, with a phonon energy $\omega^* = 260 \pm 10\ \mathrm{cm}^{-1}$, Eq. (2) provides an estimate of the polaron binding energy E_p from the line shape of the *d* band (see Fig. 5 in Ref.21). Referring to Fig. 4 of the present work, one obtains $E_p \leqslant 3\ \omega^* \simeq 780\ \mathrm{cm}^{-1}$ for sample 2, and $E_p \sim 2\omega^* \simeq 520\ \mathrm{cm}^{-1}$ for sample 3, in fair agreement with the previous determinations. The decrease of the polaron binding energy for increasing doping is consistent with the temperature dependence of the *d* band in Fig. 4(b), which becomes smoother on going from sample 1 to samples 2 and 3. Finally, the saturation temperature for the *d*-band intensity for NCO ($\approx$ 200 K) is also well accounted for by the above polaron parameters.

The energies E_j of almost all the peaks in Fig. 8 are found to be given either by $n_1\omega_1$ or by $n_2\omega_2$, for n_1 and n_2 as listed in Table II. As expected, the energies of most overtone bands are shifted with respect to their algebraic values by negative amounts due to anharmonic effects which increase with the overtone energy. If the overtones and combination bands of the two fundamentals, with linewidths γ_j given by Eq. (3) (see below), are used, the entire band can be described up to $2000\ \mathrm{cm}^{-1}$. As shown in Table II, a few of the observed IRAV's cannot be explained in terms of overtones of the two lowest local modes 1 and 2. These peaks can either be due to combination bands of 1 and 2, as suggested previously,[14] or they can be assigned to a third polaron series originating from a mode at $\omega_3 = 375\ \mathrm{cm}^{-1}$, as indicated in the same table.

In Fig. 9, the linewidths γ_j of the jth overtone in the *d* band entering the fit of the far- and midinfrared spectra of NCO sample 2 are plotted as a function of the oscillator peak energies ω_{pj}. Except for peak 2 in Fig. 8, whose anomalous broadening is possibly related to the proximity of the broad background mentioned above, the linewidths follow the phenomenological relation (solid line in the figure)

$$\gamma_j = 10 + 1.6 \times 10^{-7}\omega_{pj}^3, \quad (3)$$

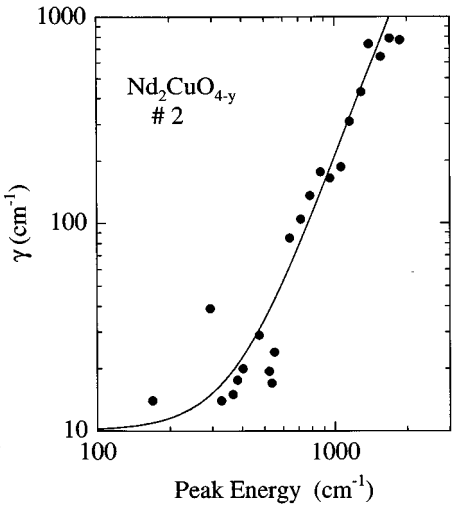

FIG. 9. Linewidth γ as a function of the peak energies for both local modes and spectral structures identified in the *d* band of NCO. The solid line is a best fit to data as explained in the text.

where γ_j and ω_{pj} are given in cm^{-1} (a smoother dependence on ω_{pj} was reported in Ref. 14, on the basis of preliminary results). As suggested by a direct inspection of data for sample 2 in Fig. 9, a discontinuity appears at $\sim 600\ \mathrm{cm}^{-1}$. At lower energies, the oscillator bands are narrow, with almost constant linewidths, while at high energies they rapidly broaden. This behavior can be explained on the basis of the small-polaron model, by assuming that the IRAV's at low energies are due to the excess electrons being localized and vibrating in a single potential well. The high-order IRAV's forming the *d* band for $\omega_{pj} > 600\ \mathrm{cm}^{-1}$ would instead promote intersite jumps of the excess charge. This situation corresponds[27] to a small polaron hopping at a frequency $t \approx E_p \approx 600\ \mathrm{cm}^{-1}$. This value is consistent with the independent evaluations of E_p presented above for sample 2 ($> 600\ \mathrm{cm}^{-1}$ and $\sim 550\ \mathrm{cm}^{-1}$). On the other hand, the small values of the low-energy overtone linewidths imply that the dispersion of the fundamental modes is small, consistent with their attribution to local vibrations. In this respect, the IRAV's here identified do not represent a single case. Several extra-phonon modes were observed by neutron scattering in $YBa_2Cu_3O_{7-y}$ (YBCO).[41] The one at 700 cm^{-1} is particularly strong and has been studied in detail. It did not show any appreciable wave vector dependence and therefore has been attributed to a local vibration.

As far as the intensities of the IRAV's are concerned, they provide further evidence for the polaronic origin of the *d* band. Indeed, the intensities of the overtones are comparable with, or even higher than, the intensities of the fundamental modes 1 and 2. As a matter of fact, the strength of vibrational overtones resulting from transitions within an anharmonic potential normally decreases by orders of magnitude as the order of the overtone increases. This is not the case for strong electron-phonon coupling. On the other hand, the LM's are produced by the introduction of a few percent of oxygen vacancies into the lattice. One can wonder how the intensities of the doping-induced local modes may be comparable with those of the extended E_u modes of the lattice. However, the charged distortion created in the lattice by the

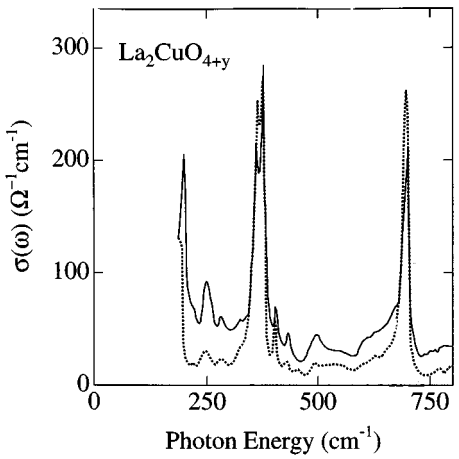

FIG. 10. $\sigma(\omega)$ at 10 K for two La_2CuO_{4+y} samples with $y<0.005$ (dotted line) and $y\simeq 0.02$ (solid line), as reported in Ref. 36.

excess carriers may induce huge local dipole moments which in turn lead to intense infrared absorption. This has indeed been predicted for the Cu-O plane in the case of strong electron-phonon coupling.[26]

The present results for the far-infrared spectrum of the *e*-doped insulators are confirmed by the $\sigma(\omega)$ reported for the *h*-doped La_2CuO_{4+y} in Ref. 42 and in Ref. 36. The latter data are shown in Fig. 10. One may notice that the onset of the *d* band is found at $\sim 600\ cm^{-1}$, as in NCO, in spite of the large difference in the phonon energies of these two materials. At lower energies, a peak at about $500\ cm^{-1}$ in LCO is the counterpart of that at $480\ cm^{-1}$ in NCO; see Fig. 7. Both these structures strongly increase for decreasing temperature and for increasing doping. The same holds for the extra-phonon peaks around $250\ cm^{-1}$.[36,42] Any closer comparison between NCO and LCO in the far infrared is made difficult by different contributions from the background in the two systems.

C. The metallic phase

It has been shown in the previous sections that IRAV's and polaronic bands are observed in the far- and the midinfrared spectra, respectively, of the insulating parent compounds of HCTS's. In the present section we extend our analysis to the metallic phase, by showing preliminary results on a *hole*-doped compound and by discussing spectra reported in the literature for both *electron*-doped and *hole*-doped cuprates. Those spectra exhibit unexpected features that are superimposed on the free-carrier absorption (Drude term). We show that in most cases these features correspond to the IRAV peaks and to the *d* band observed in the insulating cuprates. We conclude that polaron bands are likely to survive in several metallic cuprates.

Evidence for extra-Drude features in superconducting $Bi_2Sr_2CuO_6$ (BSCO) is provided in Fig. 11. The reflectivity at room temperature of a superconducting 2-μm-thick $Bi_2Sr_2CuO_6$ film ($T_c = 20$ K) is reported in the top part of the figure. The film (6) was grown by liquid phase epitaxy on $LaGaO_3$. The optical conductivity of the same sample, as obtained by Kramers-Kronig transformations of $R(\omega)$, is reported in the bottom part of the figure. As shown in Table III, the broad features superimposed on the Drude term in the far infrared have energies which correspond to those of the IRAV's found in NCO. It should be noticed that the room-temperature Drude term in the spectrum of Fig. 11 is comparable with, or weaker than, the local-mode contributions. Indeed, IRAV's should be detected more easily in systems with low carrier densities, such as for instance that of Fig. 11. The existence of extra-Drude features in this system is confirmed by the midinfrared reflectivity spectrum of a BSCO single crystal with $T_c = 10$ K, which exhibits a structured *d* band.[39]

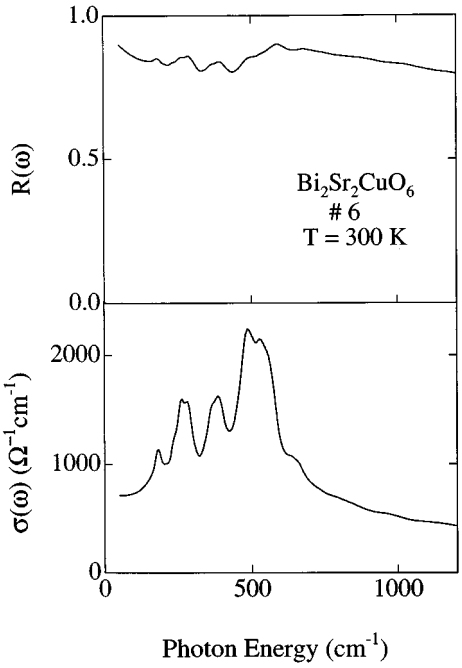

FIG. 11. Top: The room-temperature reflectivity $R(\omega)$, in the far- and midinfrared region, of a metallic 2-μm-thick $Bi_2Sr_2CuO_6$ film (6), with $T_c = 20$ K. Bottom: The optical conductivity of the same sample, as obtained by Kramers-Kronig transformations.

The *d* band at $\sim 1000\ cm^{-1}$ has already been observed in several metallic and superconducting cuprates. Indeed, it has been shown[5] that the infrared optical conductivity of metallic NCCO can be decomposed into three contributions: (i) a normal Drude term; (ii) a *d* band peaked at $\approx 1000\ cm^{-1}$; (iii) a MIR band at $\approx 4000\ cm^{-1}$. In a similar way, in four YBCO single crystals with different oxygen contents and critical temperatures T_c ranging from 30 to 90 K, Thomas *et al.*[43] have decomposed $\sigma(\omega)$ into (i) a normal Drude term; (ii) a low-energy, T-dependent contribution, peaked at $\approx 1000\ cm^{-1}$, which can be straightforwardly identified with the present *d* band; (iii) a T-independent MIR band at $\approx 5000\ cm^{-1}$. Moreover, far-infrared structures clearly appear in the low-temperature optical conductivity of the samples with $T_c = 50$ K and $T_c = 80$ K—see Fig. 8 in Ref. 44. Their energies are close to those reported here for the IRAV's of insulating NCO, as shown in Table III for the sample with $T_c = 80$ K.

Extra-Drude features can be identified also in the infrared spectra of a $Nd_{1.85}Ce_{0.15}CuO_{4-y}$ thin film[45] with $T_c = 21$ K,

TABLE III. The peak energies, in cm^{-1}, of the spectral features observed in a variety of superconducting cuprates are compared with those obtained for the local modes of insulating NCO. Data are extracted from optical conductivities, tunneling experiments, and neutron scattering experiments.

NCO 2, 3	BSCO 6	NCCO [a]	NCCO [b]	YBCO [c]	YBCO [d]	YBCO [e]
$T_c = 0$ K	$= 20$ K	$= 21$ K	$= 22$ K	$= 90$ K	$= 80$ K	$= 93$ K
Local mode						
165	180		165	165	185	168 [f]
				210	215	
	245	245			240	
282±4	270	285	270	280		
327		325	325	345	340	
366	365	370	375			
383	385					385
			415	405	405	
471	485		470	480	470	460
507		490				495
522						
536	530					
550				555	555	550
						595
641	640				625	630
717±7						700
Phonon mode						
132			125		125	

[a]From $\sigma(\omega)$, Ref. 45.
[b]From tunneling data, averaged over two different junctions, as reported in Ref. 28.
[c]From $\sigma(\omega)$, averaged over two different temperatures, Ref. 46.
[d]From $\sigma(\omega)$, averaged over different temperatures, Ref. 44.
[e]From neutron inelastic scattering, Ref. 41.
[f]From neutron inelastic scattering, $T_c = 92$ K, Ref. 47.

and of a *h*-doped, metallic[46] YBCO, with $T_c = 90$ K. A broad extra-Drude contribution, reminiscent of the *d* band, is present in both compounds with an onset at ~ 600 cm^{-1}. IRAV modes are reported in the far infrared, whose energies do not correspond to those expected for phonons in such materials. Once again, most of those IRAV energies correspond to the NCO extra modes; see Table III. Finally, in the same table we report for comparison all the modes observed by neutron scattering in YBCO,[35,41] which coincide neither with the Raman nor with the infrared phonons.

One may remark that the mode reported to occur at ~ 245 cm^{-1} in the infrared spectra of BSCO, NCCO, and YBCO is missing in the NCO spectra. As already mentioned, however, the feature at 282 ± 4 cm^{-1} in NCO exhibits an unusually large full width at half maximum (40 cm^{-1}; see Fig. 9), which could be due to the superposition of two distinct modes.

Finally, it may be worth recalling here the results of tunneling experiments on a $Nd_{1.85}Ce_{0.15}CuO_{4-y}$ sample with $T_c = 22$ K. Huang *et al.*[28] have measured at 4.2 K the spectral function $\alpha^2F(\omega)$ in two different tunnel junctions, finding maxima at the energies reported in Table III. One can easily see that those maxima coincide in energy with the infrared extra-phonon peaks found in NCO. Only accidental correspondences can be found, instead, between $\alpha^2F(\omega)$ and the infrared- or Raman-active phonons. The feature at 125 ± 6 cm^{-1}, which is not included among the IRAV's of NCO, corresponds to the lowest-energy phonon in the *a*-*b* plane of this cuprate.

IV. CONCLUSION

In the present work, evidence for the existence of polaronic infrared bands in both hole- and electron-doped insulating cuprates has been provided. These bands are peaked at ≈ 1000 cm^{-1}, like those observed in the photoinduced spectra of several parent compounds of HCTS's. Within standard one-phonon, adiabatic polaron models, they correspond to small polarons with a binding energy of ~ 500 cm^{-1}. A polaron fine structure has been partially resolved in the present spectra, similar to that predicted by recent exact calculations on small clusters. The fine structure is here explained in terms of overtones of the additional modes, depending on both doping and temperature, which appear at 165 and 282 cm^{-1} (and possibly at ~ 375 cm^{-1}) in the phonon spectrum of Nd_2CuO_{4-y}. These modes are assigned to strongly infrared-active vibrations of the lattice, locally perturbed by the excess charges. They also appear in several metallic cuprates, both *hole*- and *electron*-doped, where they are superimposed on the Drude term. In the HCTS's several

authors have also observed broad bands, dependent on temperature and centered at $\approx 1000\ \mathrm{cm}^{-1}$. These results confirm the link between the local modes in the far infrared and the *d* band. They also suggest that the polaronic behavior of the optical conductivity is a general feature of the Cu-O plane, and indicate that polarons may survive in the metallic phases of HCTS's. Therein, two types of carriers may be present, small polarons with hopping energies of the same order as the binding energy ($\approx 500\ \mathrm{cm}^{-1}$) and carriers with lower effective masses. Tentatively, the latter carriers may represent either a normal Fermi liquid coexisting with a substrate of small polarons, or the coherent part of a polaron fluid.

A crucial question obviously concerns the role polarons may play in high-T_c superconductivity. On the basis of the present results and of our interpretation of data already available in the literature, we can contribute to the debate by proposing the following two considerations.

In a previous section we have discussed recent tunneling results, which identify the lattice modes that in NCCO strongly interact with the carriers responsible for superconductivity. These modes have the same energies as the IRAV's here detected in the insulating phase. This comparison, which is meaningful as local modes have negligible dispersion in the space of momenta, suggests that in NCCO *the modes which interact most strongly with carriers in the superconducting phase are those of local origin, not the extended phonons of the unperturbed lattice*.

Secondly, one should carefully examine the infrared data taken by Thomas *et al.*[43] in YBCO samples with different T_c. In Ref. 43, it has been found that T_c increases with the effective number of carriers in the *d* band, $n_d = (2m^*V/\pi e^2)\int_0^\infty \sigma_d(\omega)d\omega$. The intensity of the MIR band was found instead to be *independent of* T_c *within errors*. Several authors[23,27] have suggested that a Bose condensation of bipolarons may account for superconductivity in HCTS's. In this case $T_c \propto n_{\mathrm{bipolaron}}^{2/3}$. If one assumes $n_d \propto n_{\mathrm{bipolaron}}$, one could wonder whether $T_c \propto n_d^{2/3}$. Indeed, from the data of Ref. 43 one obtains with a good approximation $T_c \propto (n_d/n_{\mathrm{MIR}})^{2/3}$. At present, however, we do not know whether this phenomenological argument is physically meaningful or not. In particular, one should justify the assumption that the number of effective carriers in the small-polaron *d* band is proportional to that of mobile bipolarons which would condense below T_c.

ACKNOWLEDGMENTS

We wish to thank A. Bianconi, R. Caciuffo, C. Castellani, B. Chakraverty, C. Di Castro, M. Grilli, V. Kabanov, and G. Strinati for useful discussions. G. Balestrino, H. Berger, S-W. Cheong, W. Sadowski, and E. Walker are gratefully acknowledged for providing the samples used in this work. We are also indebted to P. G. Medaglia for his collaboration. Some authors (P.C., A.P., and S.L.) wish to thank the LURE laboratory, where some of the present data have been collected. This work has been supported in part by Istituto Nazionale di Fisica della Materia of Italy and by the Human Capital and Mobility Programme of the European Union (Contract No. CT94-0551).

[1] T. Timusk and D. B. Tanner, in *Physical Properties of High Temperature Superconductors*, edited by D. M. Ginsberg (World Scientific, Singapore, 1989), pp. 339–407, and references therein.

[2] J. P. Falck, A. Levy, M. A. Kastner, and R. J. Birgenau, Phys. Rev. Lett. **69**, 1109 (1992).

[3] S. Uchida, H. Takagi, and Y. Tokura, Physica C **162–164**, 1677 (1989).

[4] S. L. Cooper, G. A. Thomas, J. Orenstein, D. H. Rapkine, A. J. Millis, S.-W. Cheong, A. S. Cooper, and Z. Fisk, Phys. Rev. B **41**, 11 605 (1990).

[5] S. Lupi, P. Calvani, M. Capizzi, P. Maselli, W. Sadowski, and E. Walker, Phys. Rev B **45**, 12 470 (1992).

[6] C. M. Foster, A. J. Heeger, G. Stucky, and N. Herron, Solid State Commun. **71**, 945 (1989).

[7] P. Calvani and S. Lupi, Solid State Commun. **85**, 665 (1993).

[8] G. A. Thomas, D. H. Rapkine, S. L. Cooper, S.-W. Cheong, A. S. Cooper, L. F. Schneemeyer, and J. V. Waszczak, Phys. Rev. B **45**, 2474 (1992).

[9] J. P. Falck, A. Levy, M. A. Kastner, and R. J. Birgenau, Phys. Rev. B **48**, 4043 (1993).

[10] A. J. Epstein, J. M. Ginder, J. M. Leng, R. P. McCall, M. G. Roe, H. J. Ye, W. E. Farneth, E. M. McCarron, and S. I. Shah, in *High T_c Superconductors*, edited by A. Bianconi and A. Marcelli (Pergamon, Oxford, 1989), p. 87; C. Taliani, R. Zamboni, G. Ruani, A. J. Pal, F. C. Matacotta, Z. Vardeny, and X. Wea, *ibid.*, p. 95.

[11] Y. H. Kim, S.-W. Cheong, and Z. Fisk, Phys. Rev. Lett. **67**, 2227 (1991); Y. H. Kim, A. J. Heeger, L. Acedo, G. Stucky, and F. Wudl, Phys. Rev. B **36**, 7252 (1987).

[12] D. Mihailovic̀, C. M. Foster, K. Voss, and A. J. Heeger, Phys. Rev. B **42**, 7989 (1990).

[13] C. Taliani, R. Zamboni, G. Ruani, F. C. Matacotta, and K. I. Pokhodyna, Solid State Commun. **66**, 487 (1988).

[14] P. Calvani, M. Capizzi, S. Lupi, P. Maselli, A. Paolone, P. Roy, S.-W. Cheong, W. Sadowski, and E. Walker, Solid State Commun. **91**, 113 (1994).

[15] P. Calvani, S. Lupi, P. Roy, M. Capizzi, P. Maselli, A. Paolone, W. Sadowski, and S.-W. Cheong, in *Polarons and Bipolarons in High-T_c Superconductors and Related Materials*, edited by Y. Liang, E. Salje, and A. Alexandrov (Cambridge University Press, Cambridge, England, 1995).

[16] A. Bianconi and M. Missori, in *Phase Separation in Cuprate Superconductors*, edited by E. Sigmund and A. K. Müller (Springer-Verlag, Berlin, 1994), p. 316.

[17] C. H. Chen, S.-W. Cheong, and A. S. Cooper, Phys. Rev. Lett. **71**, 2461 (1993).

[18] S. J. L. Billinge and T. Egami, Phys. Rev. B **47**, 14 386 (1993).

[19] B. K. Chakraverty, J. Phys. (Paris) **42**, 1351 (1981).

[20] A. Alexandrov and J. Ranninger, Phys. Rev. B **23**, 1796 (1981).

[21] D. Emin, Phys. Rev. B **48**, 13 691 (1993).

[22] S. Robaszkiewicz, R. Micnas, and J. Ranninger, Phys. Rev. B **36**, 180 (1987).

[23] J. Ranninger, Solid State Commun. **85**, 929 (1993).

[24] H. G. Reik and D. Heese, J. Phys. Chem. Solids **28**, 581 (1967);

H. G. Reik, in *Polarons in Ionic Crystals and Polar Semiconductors*, edited by J. Devreese (North-Holland, Amsterdam, 1972), and references therein.

[25] T. Holstein, Ann. Phys. (N.Y.) **8**, 325 (1959).

[26] K. Yonemitsu, A. R. Bishop, and J. Lorenzana, Phys. Rev. Lett. **69**, 965 (1992); Phys. Rev. B **47**, 8065 (1993).

[27] A. S. Alexandrov, V. V. Kabanov, and D. K. Ray, Physica C **224**, 247 (1994).

[28] Q. Huang, J. F. Zasadzinski, N. Tralshawala, K. E. Gray, D. G. Hinks, J. L. Peng, and R. L. Greene, Nature **347**, 369 (1990).

[29] C. P. Flynn, *Point Defects and Diffusion* (Clarendon, Oxford, 1972), pp. 239–268.

[30] It should be pointed out that Fig. 4(a) rules out the possibility that the *d* band might have a purely magnetic origin, as one could infer from the observation that its peak energy is close to that of a magnon propagating in these materials. Indeed, the Néel temperature in NCO is lower than 270 K for any doping level (Ref. 31) and is known to decrease rapidly in strongly reduced crystals. Therefore in no way could one explain the existence of a well defined magnonic absorption at 300 K, which, moreover, increases with oxygen reduction.

[31] S. Skanthakumar, H. Zhang, T. W. Clinton, W.-H. Lee, J. W. Lyn, Z. Fisk, and S.-W. Cheong, Physica C **160**, 124 (1989).

[32] A. J. Pal, P. Manda, A. Poddar, and B. Ghosh, Physica C **181**, 186 (1991).

[33] E. T. Heyen, G. Kliche, W. Kress, W. König, M. Cardona, E. Rampf, J. Prade, U. Schröder, A. D. Kulkarni, F. W. de Wette, S. Piñol, D. McK. Paul, E. Morán, and M. A. Alario-Franco, Solid State Commun. **74**, 1299 (1990).

[34] M. K. Crawford, G. Burns, G. V. Chandrashekhar, F. H. Dacol, W. E. Farneth, E. M. McCarron III, and R. J. Smalley, Phys. Rev. B **41**, 8933 (1990).

[35] N. Pyka, N. L. Mitrofanov, P. Bourges, L. Pintschovius, W. Reichardt, A. Yu. Rumiantsev, and A. S. Ivanov, Europhys. Lett. **18**, 711 (1992).

[36] G. A. Thomas, D. H. Rapkine, S.-W. Cheong, and L. F. Schneemeyer, Phys. Rev. B **47**, 11 369 (1993).

[37] D. Mihailovic̀, C. M. Foster, K. F. Voss, T. Mertelj, I. Poberaj, and N. Herron, Phys. Rev. B **44**, 237 (1991).

[38] T. Timusk and D. B. Tanner, Physica C **169**, 425 (1990).

[39] M. Capizzi, S. Lupi, P. Calvani, P. Maselli, A. Paolone, P. Roy, H. Berger, and G. Balestrino, Physica C **235–240**, 273 (1994).

[40] A higher value for ω_1 (183 cm^{-1}) has been determined in Ref. 14, where the background at 200 cm^{-1} has not been subtracted, although this contribution can be distinguished in the reflectivity data of Fig. 1 of Ref. 14.

[41] M. Arai, K. Yamada, Y. Hidaka, S. Itoh, Z. A. Bowden, A. D. Taylor, and Y. Endoh, Phys. Rev. Lett. **69**, 359 (1992).

[42] A. V. Bazhenov, K. B. Rezchikov, T. N. Fursova, A. A. Zakharov, and M. B. Tsetlin, Physica C **214**, 45 (1993).

[43] G. A. Thomas, S. L. Cooper, J. Orenstein, D. H. Rapkine, A. J. Millis, J. V. Waszczak, and L. F. Schneemeyer, Supercond. Sci. Technol. **4**, S235 (1991).

[44] J. Orenstein, G. A. Thomas, A. J. Millis, S. L. Cooper, D. H. Rapkine, T. Timusk, L. F. Schneemeyer, and J. V. Waszczak, Phys. Rev. **42**, 6342 (1990).

[45] R. A. Hughes, Y. Lu, T. Timusk, and J. S. Preston, Phys. Rev. B **47**, 985 (1993).

[46] K. Kamarás, S. L. Herr, C. D. Porter, N. Tache, D. B. Tanner, S. Etemad, T. Venkatesan, E. Chase, A. Inam, X. D. Wu, M. S. Hedge, and B. Dutta, Phys. Rev. Lett. **64**, 84 (1990).

[47] N. Pyka, W. Reichardt, L. Pintschovius, S. L. Chaplot, P. Schweiss, A. Erb, and G. Müller-Vogt, Phys. Rev. B **48**, 7746 (1993).